Hindawi
Advances in Civil Engineering
Volume 2018, Article ID 2352174, 16 pages
https://doi.org/10.1155/2018/2352174

Research Article

Displacement and Stress Characteristics of Tunnel Foundation in Collapsible Loess Ground Reinforced by Jet Grouting Columns

Youyun Li,[1] Shuoshuo Xu,[1] Houquan Liu,[1,2] Enlin Ma,[1] and Lixin Wang[3]

[1]*School of Highway, Chang'an University, Xi'an 710064, China*
[2]*China Railway Siyuan Survey and Design Group Co., Ltd., Wuhan 430063, China*
[3]*State Key Laboratory of Rail Transit Engineering Informatization, China Railway First Survey and Design Institute Group Co., Ltd., Xi'an 710043, China*

Correspondence should be addressed to Houquan Liu; liuhouquan@chd.edu.cn

Received 25 May 2018; Revised 1 August 2018; Accepted 6 August 2018; Published 16 September 2018

Academic Editor: Lukasz Sadowski

Collapsible loess tunnel foundation reinforcement is a new challenge in the construction process of tunnel engineering. According to the field displacement and stress monitoring of the Fujiayao loess tunnel, this paper investigates the reinforcing effect of a high-pressure jet grouting pile on a collapsible loess tunnel foundation in the deep large-span tunnel. The field monitoring method was employed to address the performance of tunnel foundation settlement, additional stress, earth pressure, rock pressure, etc. The results indicate that the stress on the pile tops and the earth pressure between piles increase gradually over time in two stages: stress increases rapidly in the first 45 days and, after this period, stress tends to gradually stabilize. Further, stress increases uniformly with the distance from the centerline of the tunnel, and the rock pressure of the tunnel sidewalls tends to be stable within two months of being constructed. Additional stress on the tunnel foundation increases linearly with time, and it is uniformly distributed in the vertical and horizontal directions of the tunnel section. Settlement of the tunnel foundation also gradually increases with time, and it tends to be stable at 50 days from the time of construction. Additionally, the settlements of different monitoring points are similar at the same depth. The research results will further improve the theoretical knowledge of tunnel bottom reinforcement in the loess tunnel, which not only can effectively guide the design and construction of the loess tunnel and reduce disease treatment cost but also can provide the necessary basic research data and scientific theoretical basis for revision of the corresponding specifications of highway tunnels and railway tunnels.

1. Introduction

In recent years, geological hazards happened frequently [1–3], and with the development of rock engineering [4, 5] and civil engineering [6–9], a substantial number of tunnel projects have been constructed in complex geological areas as western development strategies have been implemented in China [10–16]. The construction of loess tunnels has become a focus of the tunnel field, and many relevant practical experience and theoretical results have been obtained [17–23]. However, with the increasing number of loess tunnel projects, a new challenge has arisen. As the foundations of many loess tunnels were weak, problems had arisen during the tunnel construction process. Specifically, the soil of some loess tunnel foundations was not compact, or it had a high moisture content, which caused difficulty in constructing the tunnel invert. In addition, many tunnel foundations were located in collapsible loess [24, 25]; when confronted with water, these foundations would settle unevenly [26–29], which would cause further cracking in the lining structure [30–32]. Additionally, some loess tunnels swelled, making the inverted curvature difficult to maintain [33, 34]. With regard to such loess foundations, certain reinforcement measures should be taken to control excessive deformation and uneven settlement, thus ensuring the stability of the foundations. However, the construction space in a tunnel is extremely narrow, and given the poor quality of the tunnel surrounding rock [35, 36], it is necessary to reduce disturbances on the surrounding rock during the construction process. This often restricts the available reinforcement methods.

There has been some research that is relevant to the reinforcement of the tunnel foundation [37, 38]; in particular, studies have analyzed root piles [39–41], compaction piles [42], and jet grouting piles [43]. The jet grouting pile has become the most important reinforcement method for tunnel foundations, and it has become increasingly popular due to its characteristics of low cost, high construction efficiency, small disturbance, and wide application range. In addition, it has been increasingly used in soft loess highway tunnels. For instance, in the Tujiawan tunnel, jet grouting piles were used in soft loess sections with a high water content, and the foundations were found to be stable after reinforcement. In the Dayoushan loess tunnel, jet grouting piles were adopted in the loose soil sections, and they behaved as an effective control of deformations [44].

According to the previous literature, the explorations on tunnel foundation reinforcement have concentrated on railway tunnels; few studies have focused on highway tunnel foundations in general or on collapsible loess highway tunnels in particular. However, we are seeing that more and more collapsible loess foundations of highway tunnels are in need of reinforcement during the construction process. At present, owing to deficient construction experiences and theoretical research, the treatment of collapsible loess tunnel foundations was basically referred to the "Code for building construction in collapsible loess regions" [45] and "Code for design of building foundation" [46]. These guides assume that there are no differences between tunnel foundations and general building foundations. In fact, due to the bearing effect of the surrounding rock and the unloading effect of tunnel foundations, the stress is greatly different compared with general foundation engineering [47]. Hence, the foundation reinforcement of collapsible loess highway tunnels is an urgent engineering problem in tunnel construction, and it is important to explore the variations of the deformations and stress of the reinforced tunnel foundation.

Therefore, this paper investigates the Fujiayao loess highway tunnel project (a three-lane loess tunnel with large sections). According to the field monitoring data, the variations of the deformation and stress of a collapsible loess foundation reinforced by a jet grouting pile were addressed to further evaluate the reinforcing effect. This research enriches our understanding of foundation reinforcement techniques and theories of collapsible loess tunnels and makes suggestions that may further improve the quality of tunnel construction.

2. Engineering Overview

Collapsible loess tunnel foundations settle unevenly when confronted with water, leading to further cracking in the tunnel liner. Additionally, some loess tunnels swell during construction, and the inverted curvature is difficult to maintain. In the case of weak loess tunnels, significant deformation not only occurs in the construction stage but also during tunnel operation when reinforcement is not applied.

The Fujiayao tunnel, the first three-lane super-large section tunnel in Gansu province, is located in Zhonghe Town in Gaolan County on the north bank of the Yellow River in Lanzhou city. The tunnel is 1532 m in total length of double lines with a maximum buried depth of 112 m. The tunnel excavation area is more than 170 m^2 with 17 m in excavation width and 11 m in excavation height, and the grade of the surrounding rock in this tunnel is V [48]. The tunnel passes through the loess ridge; the entrance of the tunnel is at one side of the loess gully, and the exit is at the right of the upstream of Qiujiagou. The strata in the tunnel site include alluvial and diluvial loess-like sandy silt Q_4^{al+pl} of the Holocene Quaternary system, eolian loess Q_3^{eol} of the Upper Pleistocene, and alluvial loess-like mingled fine sand layer Q_3^{al} of the Upper Pleistocene. At this site, the caves in loess are developed and most of them are connected with a diameter of 1.0~6.0 m and a depth of 1.5~2.0 m. Simultaneously, many of these caves are being actively developed. In the rainy season, surface water will often infiltrate downward along the caves into the tunnel area, which may greatly impact the safety of the tunnel. Moreover, collapsible loess is developed with a relatively large thickness in the tunnel area. In engineering characteristics, collapsible loess belongs to a metastable structure which can withstand high vertical loads with a small amount of settlement at dry, but this soil is particularly susceptible to certain water conditions, which shows an upsurge in settlement, a plunge in load capacity upon wetting and contributes to a safety hazard for infrastructures constructed in this region [49–51]. The collapsible thickness of general eolian loess Q_3^{eol} is 0~20 m, with Grade II-III self-weight collapsibility. The collapsible thickness of alluvial loess-like soil Q_3^{al} is 10~20 m, with Grade I-II non-self-weight collapsibility generally. Finally, the aquifer lies below the designed elevation of the tunnel, and the surrounding rock is generally dry to slightly wet. The longitudinal profile of the tunnel is shown in Figure 1.

3. Finite Element Analysis of Jet Grouting Pile

3.1. Finite Element Model and Selected Parameters. To investigate the effect of the jet grouting pile, based on the MIDAS-GTS (geotechnical and tunnel analysis system) software, a finite element model with a size of 80 × 70 m was developed, as shown in Figure 2. Elastoplastic materials were used for simulating the soil layers. Beam elements were employed to simulate the vertical jet grouting piles. The implantable truss elements were used for the bolts. The interaction elements between the pile and soil were constructed for a better simulation of the contact situation; the pile end and pile interface elements were selected as interaction elements. The mixed mesh is used in the model. The fixed vertical movements were set at the bottom boundary in this model; the top boundary was set to be free at the ground surface, and the horizontal movements at either side were set at zero. In total, the model consists of 9002 elements and 9052 notes. Without compromising accuracy, a coarse mesh was used at the far boundaries, whereas a fine mesh was used for the key sections (i.e., the tunnel). Simultaneously, the previous three-dimensional model was based on the following assumptions:

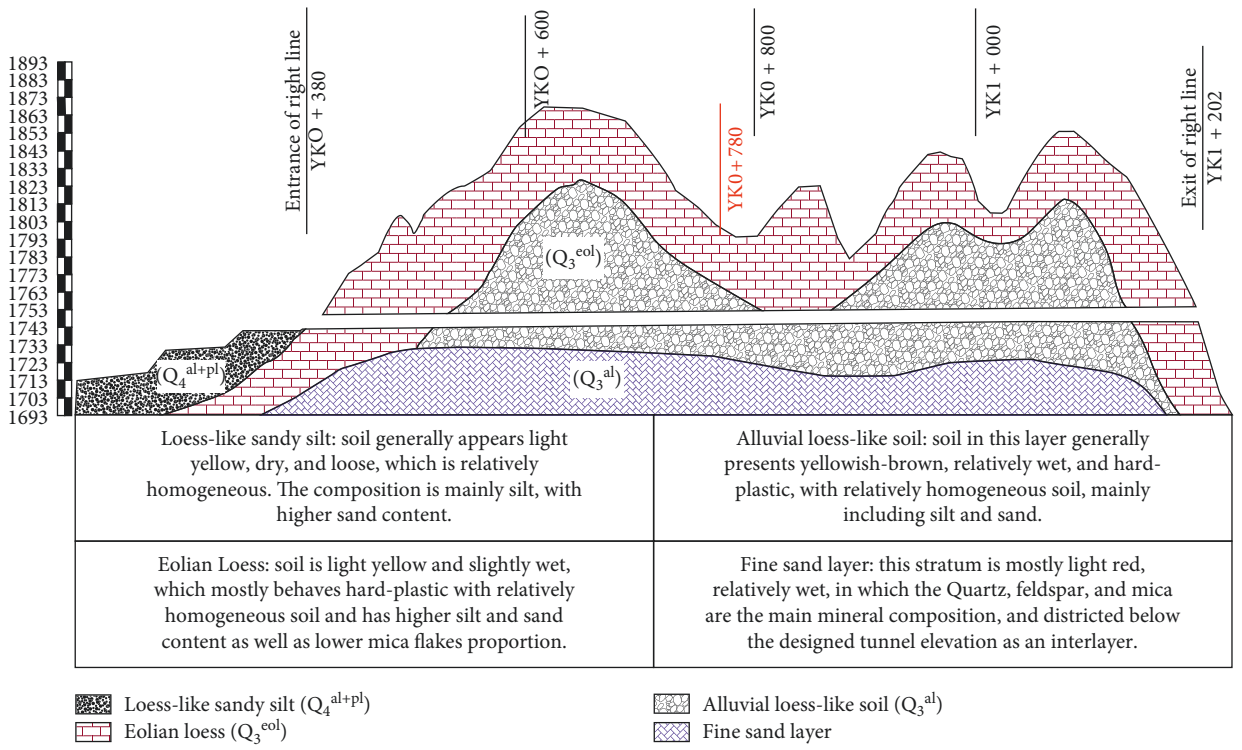

Figure 1: Longitudinal section of the Fujiayao tunnel.

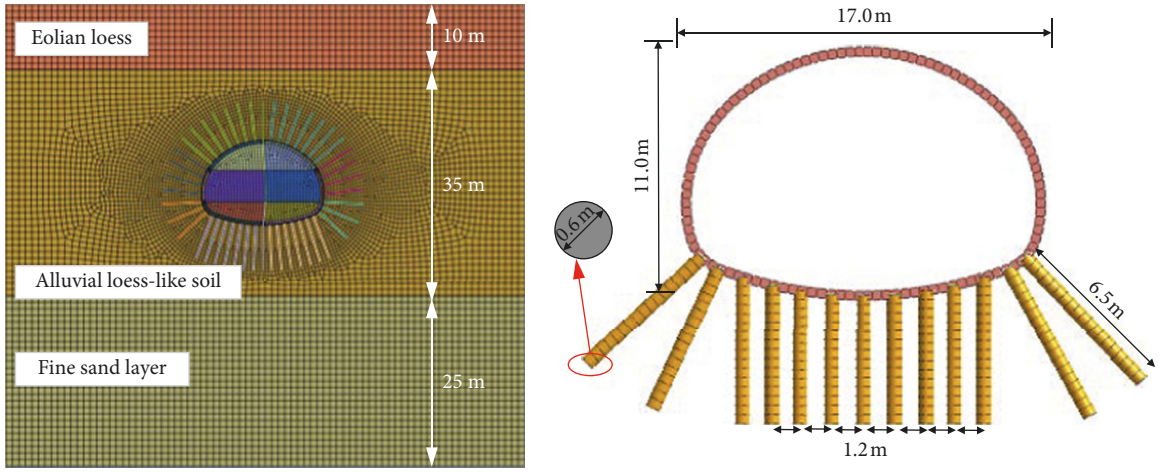

Figure 2: Mesh model and jet grouting pile element.

(1) All materials in this model are homogeneous, continuous, and isotropous

(2) Solid elements with elastoplastic materials are subjected to the Mohr-Coulomb criterion condition

(3) The beam elements, implantable truss elements, and solid elements with elastic materials are submitted to the elastic criterion condition

Two contrastive models were developed: one adopted the jet grouting pile and the other did not. The simulation adopted the center diaphragm (CD) method. From the bottom to the top of the model, the soil profiles consist of eolian loess, alluvial loess-like soil, a fine sand layer in which the depth of eolian loess is 10 m, that of alluvial loess-like soil is 35 m, and that of the fine sand layer is 25 m. The thickness of the primary support is 20 cm, and the secondary lining is 50 cm. There are 13 piles in total, the length of the pile is 6.5 m, the pile diameter is 0.6 m, and the pile spacing is 1.2 m. The width of the tunnel is 17 m, and the height is 11 m. Soil layer parameters were acquired from the field test, and the pile parameters were typical values. The geotechnical

Table 1: Parameters used for numerical simulations [52].

Types	Elastic modulus /MPa	Poisson's ratio	Volumetric weight (kN/m^3)	Cohesion (kPa)	Angle of internal friction (°)	Permeability coefficient (cm/s)
Eolian loess (Q_3^{eol})	27	0.35	13.8	22	28	0.16×10^{-4}
Alluvial loess-like soil (Q_3^{al})	60	0.3	15.2	27	30	0.11×10^{-4}
Fine sand layer	180	0.3	18	2	32	0.32×10^{-2}
Concrete backfill	120	0.2	19	—	—	0.1×10^{-4}
Primary support	23000	0.2	23	—	—	0.39×10^{-7}
Secondary liner	25000	0.2	25	—	—	0.13×10^{-8}
Bolts	200000	0.3	78.5	—	—	—
Vertical jet grouting piles	1200	0.2	21	—	—	—

properties of jet grouting piles and soil layers are summarized in Table 1.

3.2. Numerical Results of Contrastive Model. Figure 3 shows the results of the vertical displacement after completion of excavation. There are two excavation conditions: one adopts the jet grouting pile and the other does not. Under two conditions, the results present the phenomenon of vault settlement and inverted arch uplift. As shown in Figure 3(a), the maximum uplift value of the invert reaches 85 mm, and the maximum settlement value of the vault reaches 60 mm when the jet grouting pile is not adopted to reinforce foundation. As shown in Figure 3(b), the maximum uplift value of the invert reaches only 10 m, and the maximum settlement value of the vault reaches only 9 mm when the jet grouting pile is adopted. With comparison, the jet grouting pile shows a good reinforcement effect, and the settlement of the vault and inverted arch uplift reduces to 75 mm and 51 mm, respectively.

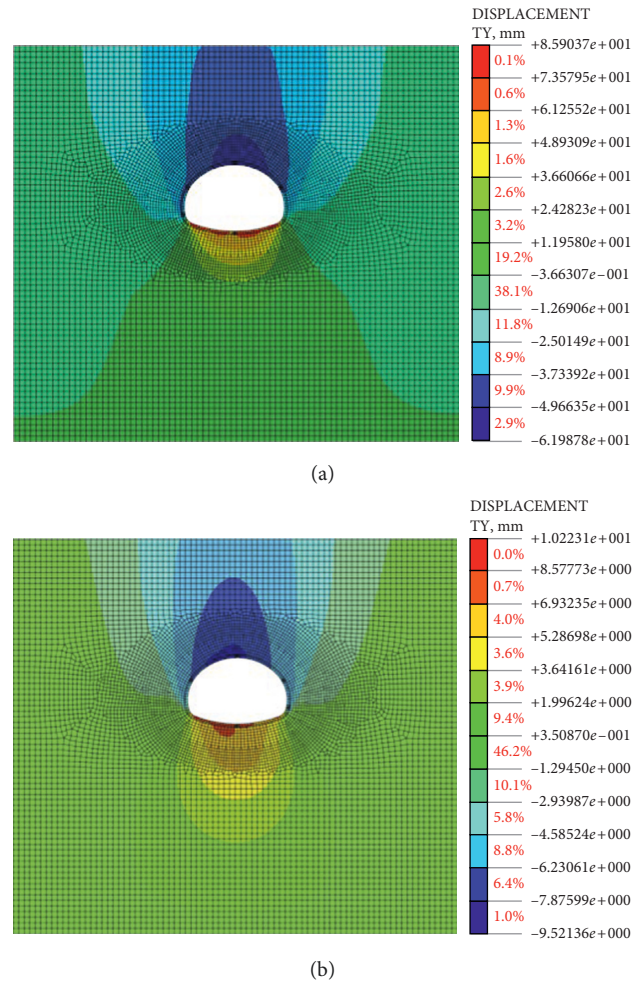

Figure 3: Vertical displacement under two conditions.

4. Reinforcement Program

During tunnel construction in a collapsible loess area, significant differential settlement of the tunnel foundation frequently occurs, which has a great influence on the structure of the tunnel. Further, in the tunnel operation stage, changes in the water environment around the tunnel may cause the tunnel foundation to develop a large collapsible deformation, which may in turn cause serious damage to the tunnel lining structure, such as ring-shaped and longitudinal cracking [53, 54]. Therefore, it is necessary to reinforce these foundations to ensure the stability of the tunnel structure. According to the requirements listed in "Code for building construction in collapsible loess regions," for class-A buildings, all collapsible settlements in the foundation should be eliminated or the pile should be employed to penetrate the collapsible loess layer to a stable soil layer [54]. For the Fujiayao tunnel, given the *in situ* conditions, the jet grouting pile was ultimately used to reinforce the foundations.

The design parameters of the jet grouting pile used in the Fujiayao tunnel are as follows: the jet grouting pile was 0.6 m in diameter and 6~7.2 m in length, which was 6 m at the center and increased outward gradually. The piles were arranged in the shape of a quincunx, with a pile spacing of 1.2 m. In addition, the center diaphragm (CD) method was employed to construct the deep section of the tunnel. The jet grouting piles were built after the construction of the supporting structure of the upper heading had been completed. The construction process of the field test mainly includes positioning of the driller, drilling, intubation, injection operation, washing operation, and waste pulp treatment. After pile construction, it was possible to excavate the heading at the lower section. The deviation between the position of the borehole and the design position shall not exceed 50 mm. Also, to guarantee the length of the piles, the nozzle lifting speed, dusting

time, and mixing time during the pile construction were strictly controlled. The upper part of the pile (1/3 pile length) must be stirred two times to ensure the quality of the pile body. On the basis of actual conditions of soft loess tunnel foundations, the allowable range of post-construction settlement is 20~40 mm. When the difference in the bearing capacity of the foundation is large, the lower limit (20 mm) should be the goal, while if the bearing capacity is distributed uniformly, the upper limit (40 mm) may be acceptable. In addition, the differential settlement should be less than 100 mm/10 m. The main construction equipment include (1) the BGP90/50-90-type high-pressure grouting pump, the grouting pressure reaches 20 MPa, and (2) the HT-150-type drilling. The construction parameters of the jet grouting pile were obtained from the field pile test, and these are summarized in Table 2. The arrangement of the piles is shown in Figure 4. Figure 5 presents data about pile construction at the site.

Table 2: Construction technology parameters of single pipe rotary jet grouting.

Type	Parameter's value
Water-cement ratio	1 : 1
Pressure (MPa)	20
Flow rate (L/min)	80~120
Nozzle diameter (mm)	1.6
Outer diameter of the rotary nozzle (mm)	42
Lifting speed (cm/min)	20~25
Rotation speed (r/min)	20~22

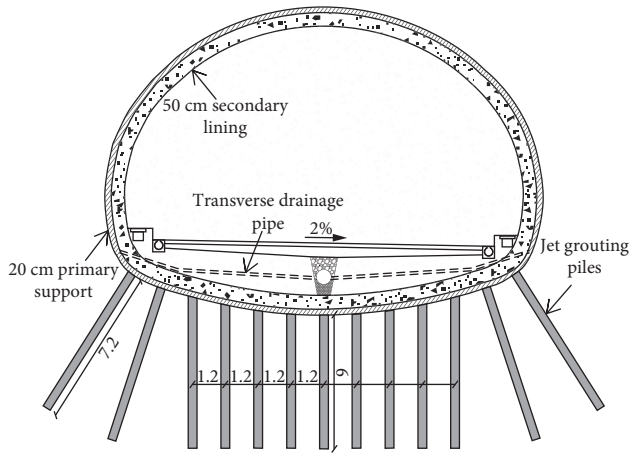

Figure 4: Design of the vertical jet grouting piles (m).

Figure 5: Construction of vertical jet grouting piles.

5. Field Monitoring

5.1. Monitoring Design. To investigate the behavior of reinforced loess tunnel foundations, different measuring points with the corresponding test instruments were laid at the typical cross-sectional locations to test the stress and deformation. Specifically, earth pressure cells were used to monitor the stress on the pile top, the earth pressure between the piles, the pressure of the surrounding rock, and the additional stress on the tunnel foundations, as shown in Figure 6. The layered displacement meters were employed to monitor foundation settlement (cf. Figure 7). Additionally, considering the closeness of the pile spacing, earth pressure cells that tested pile tops and soil between piles' stress were buried at the interval of one pile. The earth pressure cells were symmetrically arranged on both sides of the tunnel, where seven monitoring instruments were set at the pile tops and six were set in the soil between piles. To explore the pressure changes experienced in the reinforced sidewalls in the surrounding rock, three monitoring points with earth pressure cells were laid outside the primary lining on both sides to measure the surrounding rock pressure. To obtain the distribution law of additional stress on the foundation, nine measuring positions were symmetrically arranged in the tunnel, where the depth of the measuring hole was 6 m and the pressure cells were set at 2 m intervals. In addition, layered displacement meters were symmetrically arranged in the tunnel, and the depth of the measurement point was 6 m with a spacing of 5 m; in all, 4 layered displacement meters were laid with 2 m spacing. We monitored the site for 6 months with different time intervals. In the first month and a half, we obtained the data once a day; for the next month and a half, we collected data once every three days. For the final three months, we took data once a week. The data from the different monitoring sections were processed, and the results of each monitoring section were compared. We found that the data form all of the different monitoring sections were similar. Therefore, in this paper, we selected the data from a typical section YK0 + 780 to discuss the variation of stress and deformation.

5.2. Analysis of the Stress of the Pile Top and the Soil between the Piles. Figure 8 presents the variation of the stress on the pile tops over time. Stress increases rapidly in the early stages (i.e., shortly after the foundation is constructed) and then gradually becomes stable and only increases very slowly. In the first 45 days after construction, most of the stress increments have been completed. Also, stress on pile tops fluctuates somewhat in the early stages, mainly because of local damage during the compression process by uneven

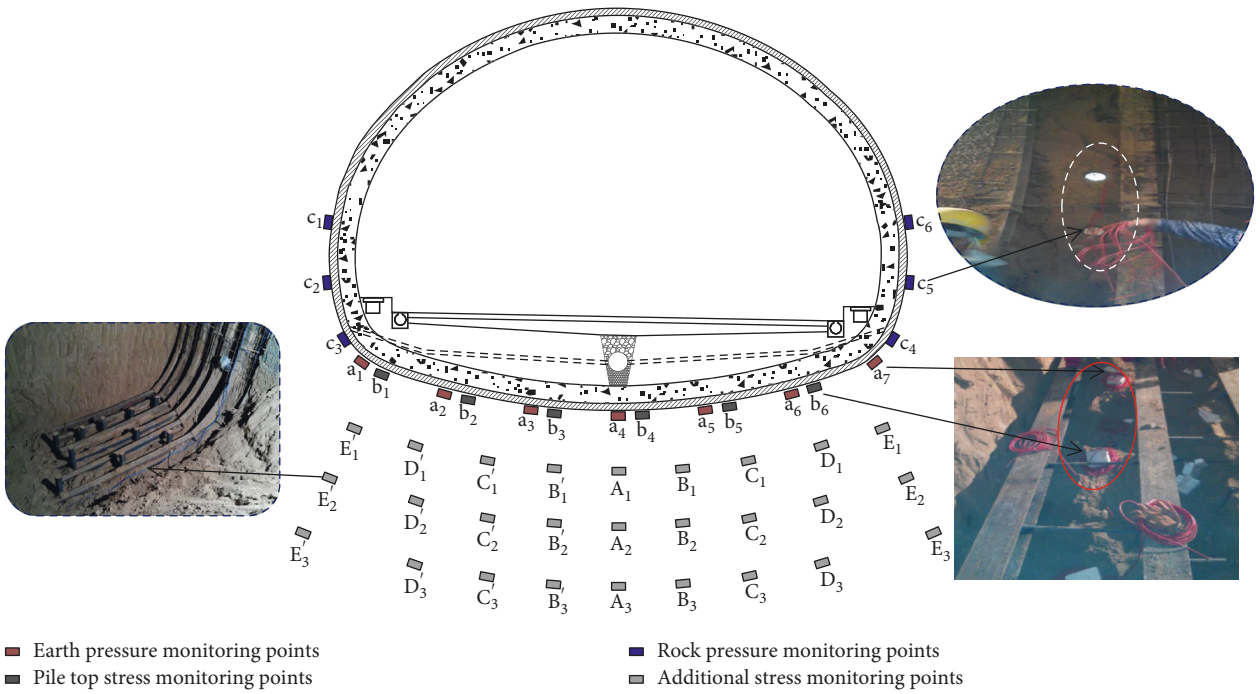

Figure 6: Layout of the earth pressure cells.

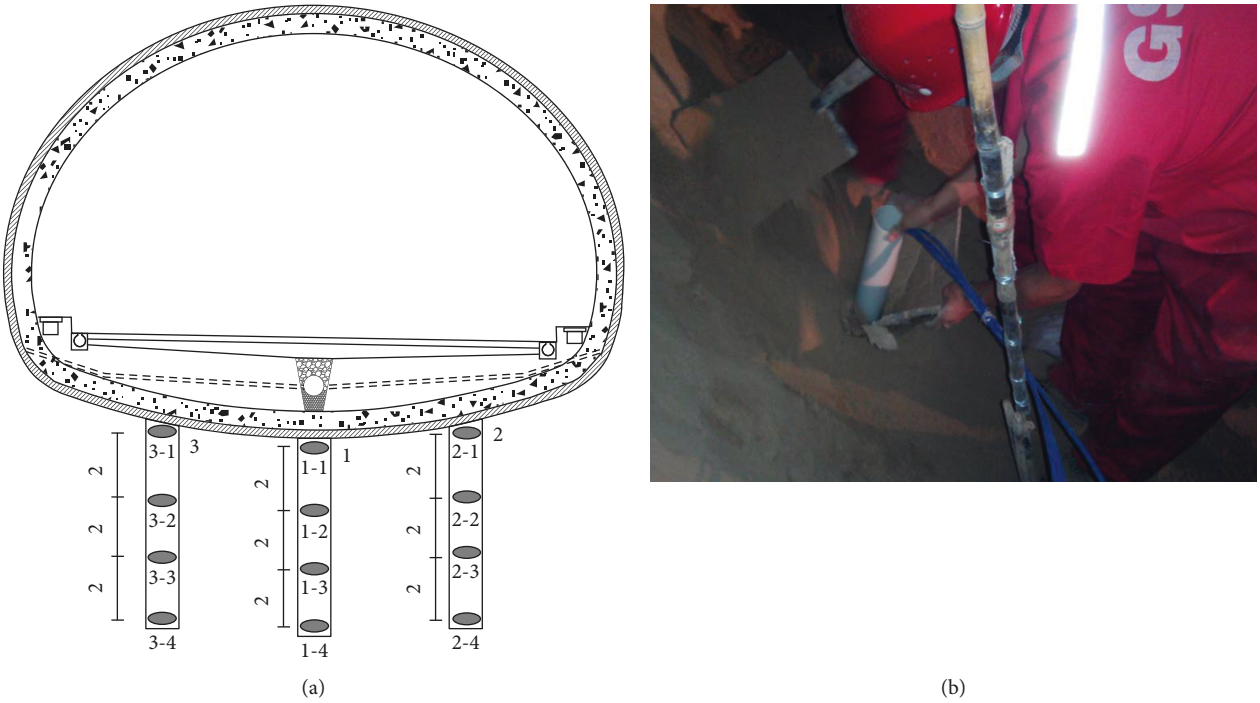

Figure 7: Layout of the layered displacement meters. (a) Arrangement of the layered displacement meters (m). (b) Buried layer displacement meters.

contact between the surface of the pile tops and that of the invert bottom.

The stable stress values (i.e., last monitored value) of each measuring point were selected to study the distribution of stress, as shown in Figure 9. The stress on the pile tops is found to be symmetrically distributed around the tunnel centerline, which increases with the distance from the tunnel centerline. In addition, the monitoring point 1-1 experiences the maximum stress value of 298 kPa, while a stress value of 85 kPa found at monitoring point 1-4 being the minimum. Stress on other pile tops is above 150 kPa, and the average pile top stress is approximately 180 kPa.

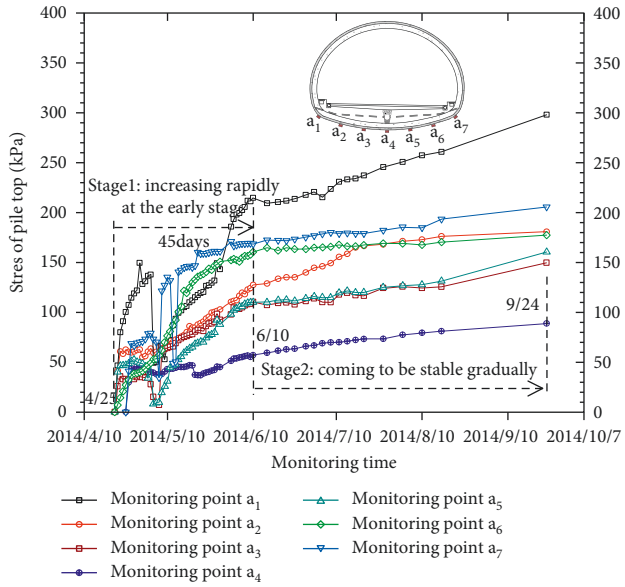

Figure 8: Variation of the stress on pile tops with time.

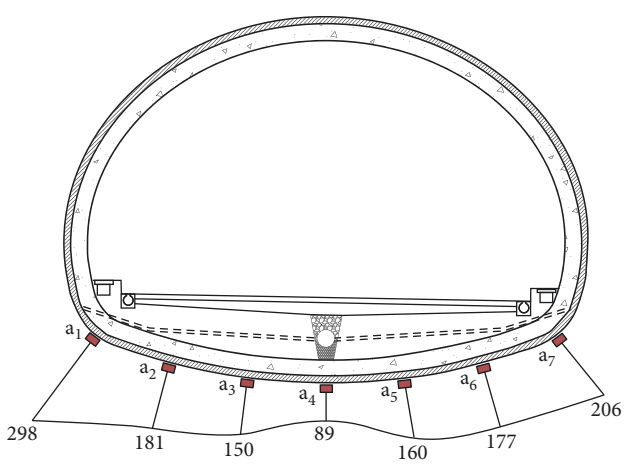

Figure 9: Distribution of the stress on pile tops (kPa).

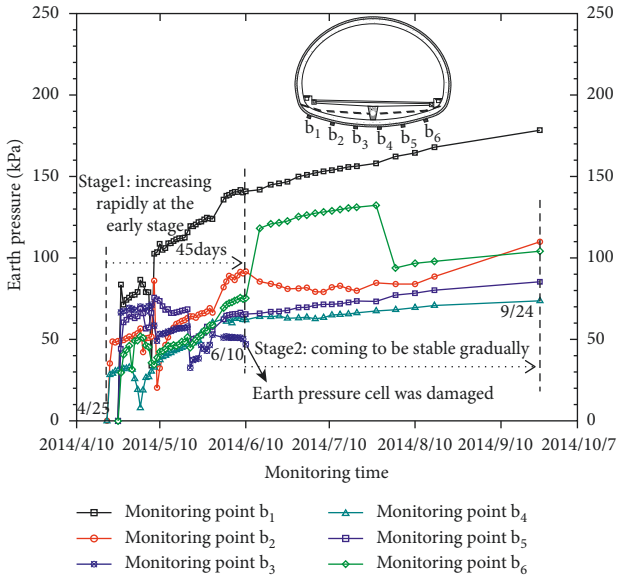

Figure 10: Variation of the earth pressure with time.

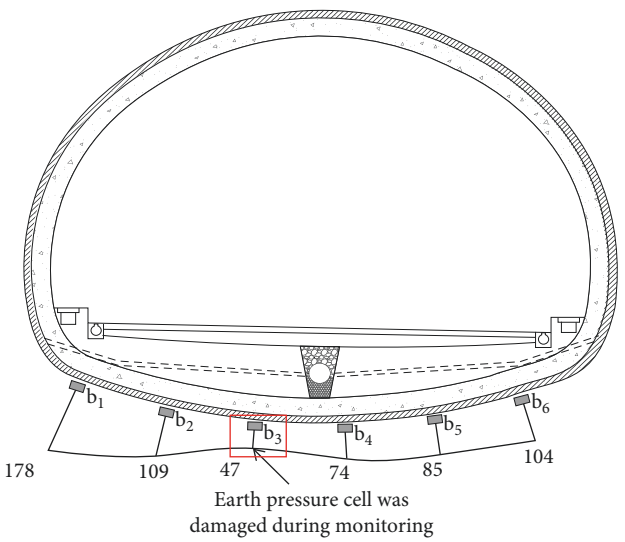

Figure 11: Distribution of the earth pressure (kPa).

The stress on the pile top is related to the position of the pile foundation and is also affected by the roughness of the inverted excavation surface. Because the inverted area was excavated using the machine, the excavation surface was not smooth, and the roughness impacts the stress on the pile tops.

The monitored results of the earth pressure between the piles are shown in Figure 10. The change laws of the earth pressure are similar to those that characterize the stress on the pile tops. The earth pressure increases gradually over time, rising sharply at first and then stabilizing gradually. Because of the failure of some monitoring instruments, the data of monitoring point b_3 are incomplete. As shown in Figure 11, the earth pressure is smaller at the center of the tunnel foundation but larger at both sides. The integral distribution of the earth pressure is uniform, which is also analogous to the pile top stress. The maximum earth pressure is 178 kPa, and the minimum value is 47 kPa. The earth pressure of other monitoring points is between 70 and 110 kPa, and the average stress is about 110 kPa. Although the earth pressure fluctuates during the construction process, it tends to be stable with time. Furthermore, the earth pressure is relatively small and uniform, without local stress concentrations. These results demonstrate that jet grouting piles can effectively control collapsible loess tunnel foundations.

The variation in the pile-soil stress ratio is illustrated in Figure 12. Affected by the construction, the pile-soil stress fluctuates greatly in the first two months after construction and then tends to be stable, exhibiting only small changes. The stable pile-soil stress ratio is at 1-2, and it is smaller at the tunnel center and larger at the sidewalls. Above all, the pile and soil stress is found to be relatively uniform, with further demonstration that the jet grouting pile provides significant reinforcing support.

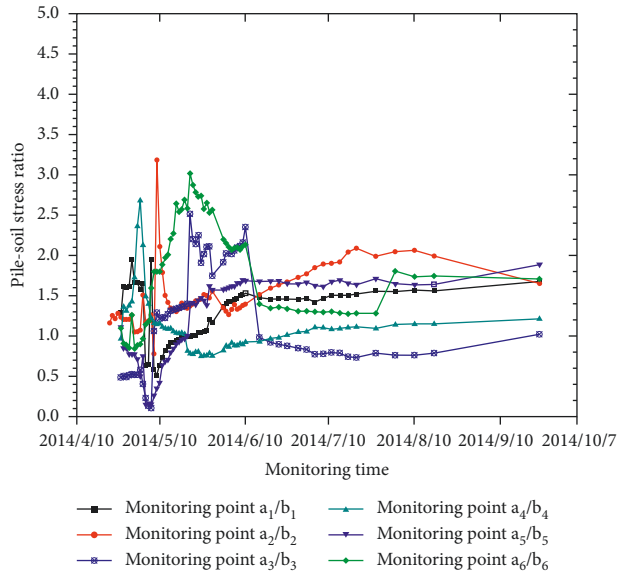

Figure 12: Variation of the pile-soil stress ratio with time.

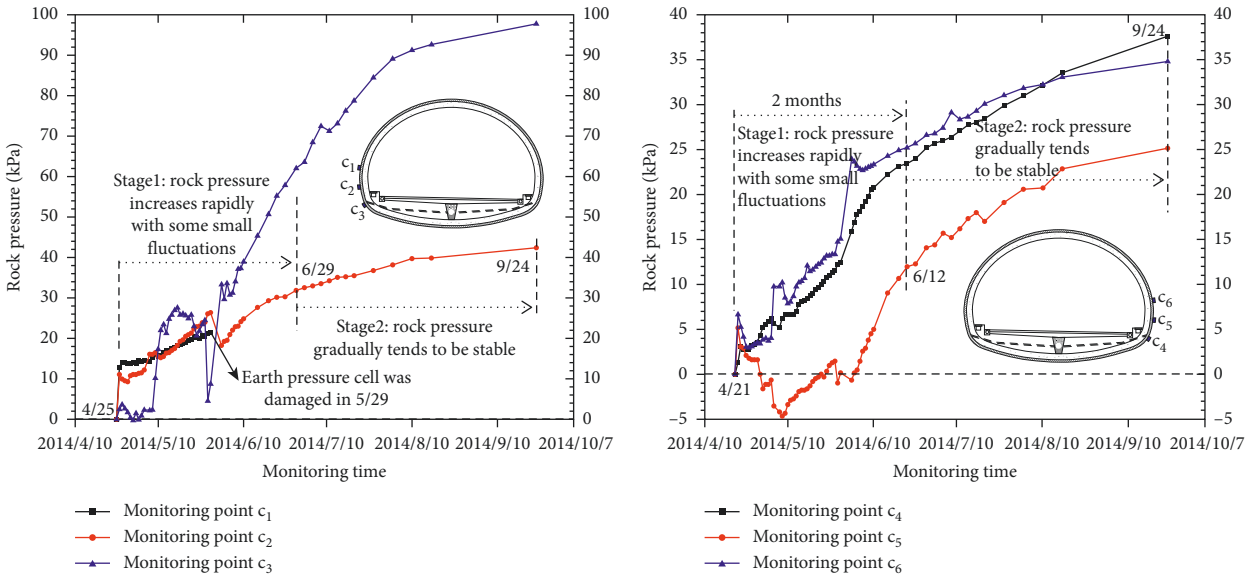

Figure 13: Variation of the rock pressure with time. (a) Left sidewall. (b) Right sidewall.

5.3. Analysis of Sidewall Surrounding Rock Pressure. The monitored results of the pressure on the sidewall surrounding rock are shown in Figure 13. This pressure increases rapidly at the early stages and then gradually gets stabilized. However, compared with the pile and soil stress, the surrounding rock pressure takes longer time to stabilize—nearly two months. Monitoring point C_3 required the longest stabilizing time—three months. Those monitoring results agree well with the results reported in [55]. At the right sidewall of the tunnel, the surrounding rock pressure is 37.6 kPa, 25.2 kPa, and 34.8 kPa from bottom to top, respectively, compared to the values of 97.8 kPa, 42.4 kPa, and 21.4 kPa at the left sidewall. The surrounding rock pressure is comparatively small (between 25 and 100 kPa in general). The pressure at the connection position between the tunnel and the invert surface is relatively larger. The pressure cell at point C_1 was damaged during the monitoring period, causing the surrounding rock pressure to be low. Finally, because it was affected by tunnel construction, the pressure curve behaves with a certain fluctuation in the early stages of construction.

5.4. Analysis of Additional Stress of Tunnel Foundation. The additional stress on the tunnel foundation increases approximately linearly and slowly with time. The stress curve

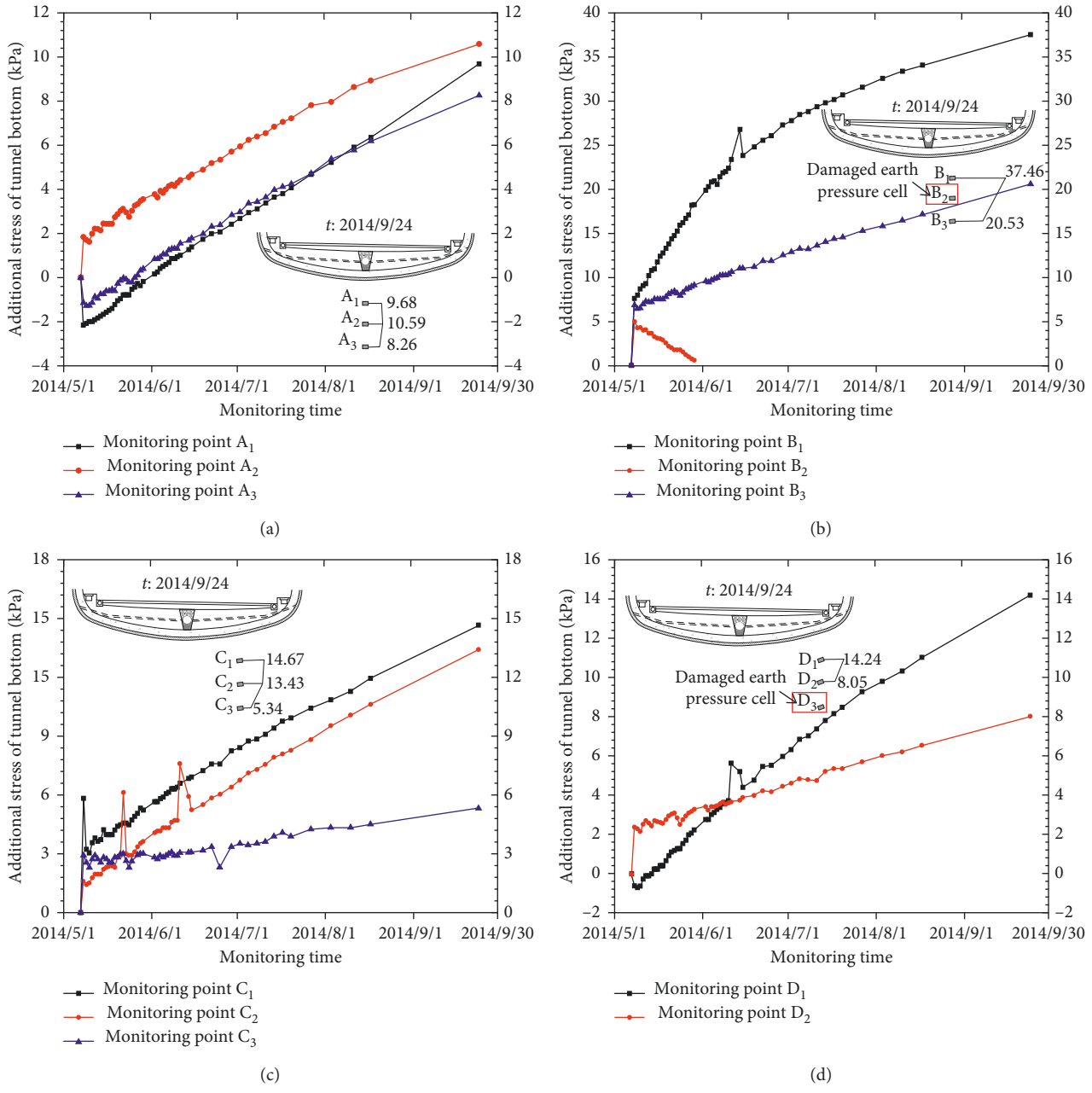

Figure 14: Continued.

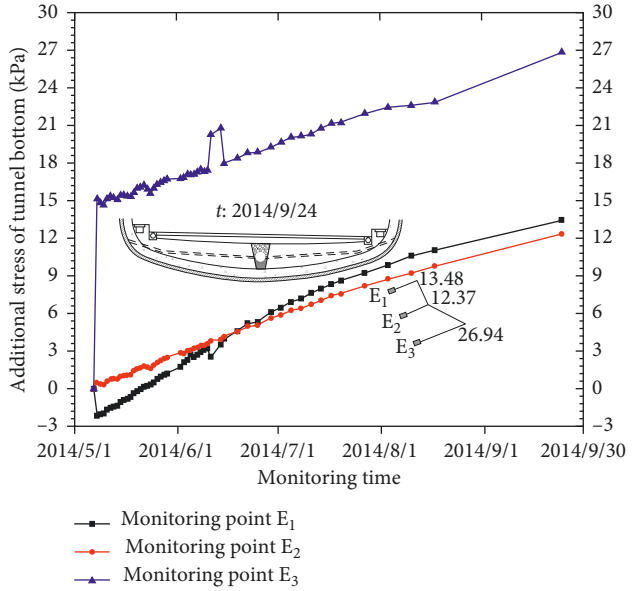

(e)

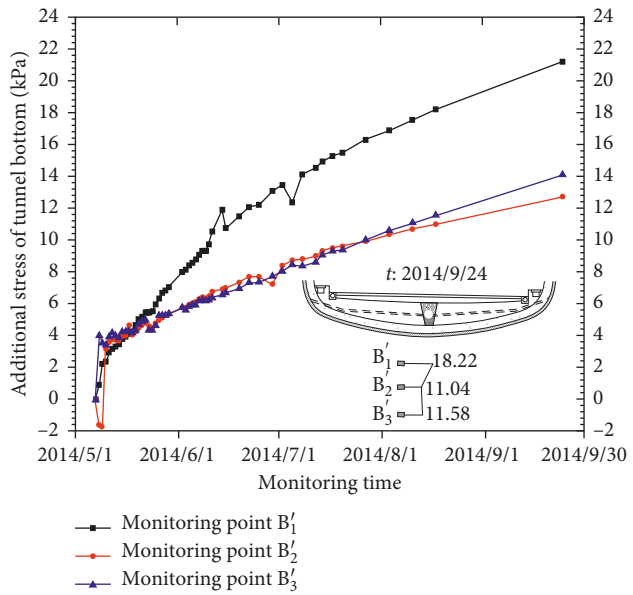

(f)

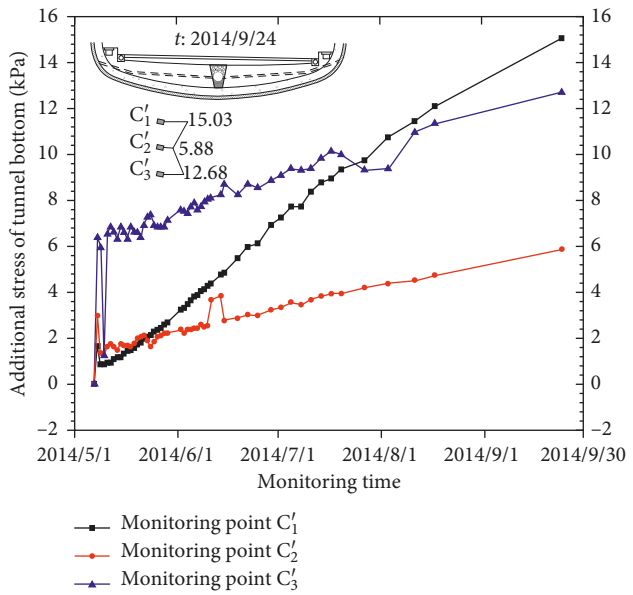

(g)

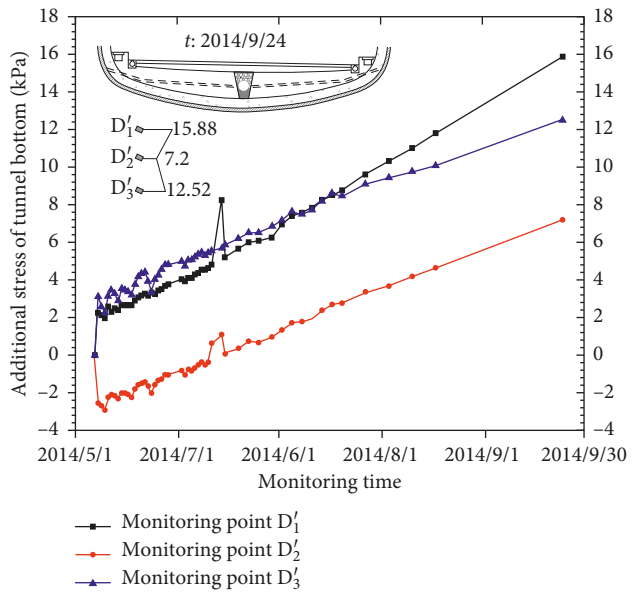

(h)

Figure 14: Continued.

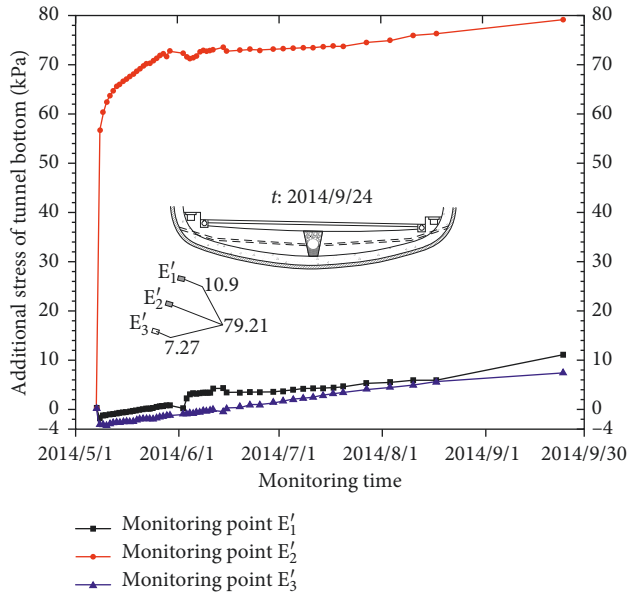

(i)

Figure 14: Variation of the additional stress on the tunnel foundation with time. (a) Monitoring point A. (b) Monitoring point B. (c) Monitoring point C. (d) Monitoring point D. (e) Monitoring point E. (f) Monitoring point B′. (g) Monitoring point C′. (h) Monitoring point D′. (i) Monitoring point E′.

changes in a stable manner with comparatively small fluctuations during the monitoring process (cf. Figure 14). Also, the increments of the additional stress at each monitoring point are small, and some curves tend to be stable in the later stages, which suggests the stability of the reinforced foundation. Additional stress recorded at some monitoring points firstly increases and then decreases as the depth increases. At the other monitoring points, the stress decreases first and then increases. The additional stress at the middle of the tunnel is more uniform, displaying a stress difference of 2.33 kPa and reaching a maximum value of 71.14 kPa at the connected position between the left invert and the sidewall. Apparently, the closer the monitoring point is to the middle of the tunnel, the smaller the stress difference is and the more uniform the stress is.

The final values for the additional stress on the tunnel foundations recorded at each monitoring point are selected and are shown in Figure 15. The additional stress is distributed uniformly along a cross-sectional direction. Except for monitoring point E'_2, the additional stress found at the other measuring points fluctuate slightly at the cross section of the tunnel. The maximum additional stress value of 79.2 kPa appears at monitoring point E'_2, and the stress value of the other measuring points fluctuates between 0 and 30 kPa. Therefore, it is evident that the additional stress experienced by a reinforced tunnel foundation is small and uniform across different depths.

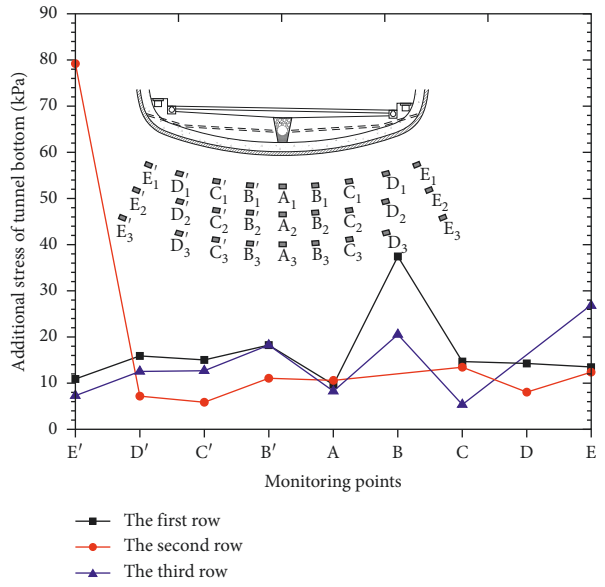

Figure 15: Distribution of the additional stress at the tunnel bottom.

5.5. Analysis of Postconstruction Settlement of Tunnel Foundations. To date, there have been no definite provisions regarding postconstruction settlement of tunnels in China, although it is generally understood that postconstruction settlement problems in various geological tunnels are more serious in soft loess tunnels [56]. Too much postconstruction settlement is liable to cause uneven settlement, which leads to further failure of the lining structure. In some domestic loess highway tunnels, the lining cracked when postconstruction settlement reached 20 mm. According to the surveys on postconstruction settlement in numerous loess tunnels, if postconstruction settlement exceeds 40 mm, tunnels would suffer from cracking of the lining or

pavement. On the basis of actual conditions of soft loess tunnel foundations, the allowable range of postconstruction settlement is 20~40 mm. When the difference in the bearing capacity of the foundation is large, the lower limit (20 mm) should be the goal, while if the bearing capacity is distributed uniformly, the upper limit (40 mm) may be acceptable. In addition, the differential settlement should be less than 100 mm/10 m.

Based on the monitoring data, we found that settlement increases gradually with a small rate of growth (cf. Figure 16). The maximum settlement of the tunnel foundations is 7.3 mm according to the monitoring point 3-4, and the settlement of the other monitoring points is less than 6 mm. The settlement of most measuring points increases rapidly during the early stages and then tends to gradually stabilize over a period of approximately 50 days, which accords with the results reported in [57–59]. Some monitoring points exhibit some swelling deformation in the early stages. It is found that the settlement of the reinforced tunnel foundation is small and stable, which suggests that the jet grouting piles effectively control the settlement of the foundations and have improved its strength. However, although the variation of settlement at various depths differ among the measuring points, settlement is relatively uniform in the vertical direction. Settlement values at different monitoring points are similar at the same depth, displaying a settlement difference (for different depths) of 1.5 mm, 4.3 mm, 3.5 mm, and 4.6 mm, respectively. These results demonstrate that the settlement of reinforced foundations is uniformly distributed with no uneven settlement, and the jet grouting pile plays an important role in protecting the lining of soft loess tunnel foundations.

6. Discussions

Some measurement points were selected to analyze the relationship between the settlement and the additional stress of tunnel foundations, as shown in Figures 17 and 18. In the depth direction, the change law between the settlement and the additional stress of the measured point in the middle and the left is the same; the settlement of the point where the stress is large is also large. The measured points on the right side do not conform to this rule; this may be due to the stress concentration which is caused by the damage of the upper part of the jet grouting pile. With the increase in depth, the change of single factor (stress or settlement) is not regular, this may be due to the lack of data. The relationship between settlement and additional stress needs further exploration.

Prior work has documented the difficulty of tunnel construction in collapsible loess areas, and many measures of tunnel foundation reinforcement have been applied to practice, for example, root piles, compaction piles, and jet grouting piles. However, these studies have not focused on the concrete displacement and stress characteristics of the tunnel foundation. In this study, we investigate the effect of the jet grouting pile by numerical simulation, and field observations were carried out to analyze the reinforcing effect of the jet grouting pile on collapsible loess tunnel foundations. We found that the surrounding rock pressure, additional stress, and settlement of the tunnel foundation increase gradually with time. This study therefore indicates that the change regulation of the surrounding rock pressure, additional stress on tunnel foundations, and settlement of the tunnel foundation were reinforced by the jet grouting pile. Our current findings expand prior work which demonstrated that jet grouting piles show effective control of the collapsible loess tunnel foundations. And the results are encouraging and should be validated in a more contrastive study.

7. Conclusions

(1) The variations of stress on pile tops are similar to those of the earth pressure on the soil between piles, which mainly occurs in two stages. In the first 45 days, the stress occurs approximately 95%, and it occurs rapidly. After this period, stress gradually decreases and becomes more stable. Also, the stress on pile tops and the earth pressure increase uniformly with the distance from the tunnel centerline.

(2) According to the monitored results, the maximum stress on the pile top is 298 kPa, and the average value is 180 kPa; the earth pressure between the piles is 178 kPa and 110 kPa, respectively. The pile-soil stress ratio fluctuates greatly in the early stage but tends to be stable 1~2 two months later.

(3) The surrounding rock pressure on the sidewalls increases rapidly at the early stage and then gradually stabilizes in approximately two months; it reaches about 70% of the maximum surrounding rock pressure. The surrounding rock pressure is comparatively small when reinforced by jet grouting piles; it is between 25 and 100 kPa in general. The pressure at the connections between the tunnel and the invert is relatively larger.

(4) The additional stress on tunnel foundations increases approximately linearly with a comparatively low fluctuation during the monitoring process. The additional stress at the middle of the tunnel is more uniform, with a stress difference of 2.33 kPa. Stress differences are lower, and stress is more uniform near the middle of the tunnel. Additional stress is distributed uniformly along a cross-sectional direction and fluctuates between 0 and 30 kPa. That is to say, the additional stress of the reinforced tunnel foundation is small and uniform at different depths.

(5) The settlement of the tunnel foundation increases gradually with a low growth rate and then gradually stabilizes in approximately 50 days. The maximum settlement of the tunnel foundation is found to be 7.3 mm, and the settlement of the other monitoring points is less than 6 mm, which reveals that the jet grouting piles help to control foundation settlement and improve the strength of the foundation. Settlement values at the different monitoring points are closer together when the points are at the same

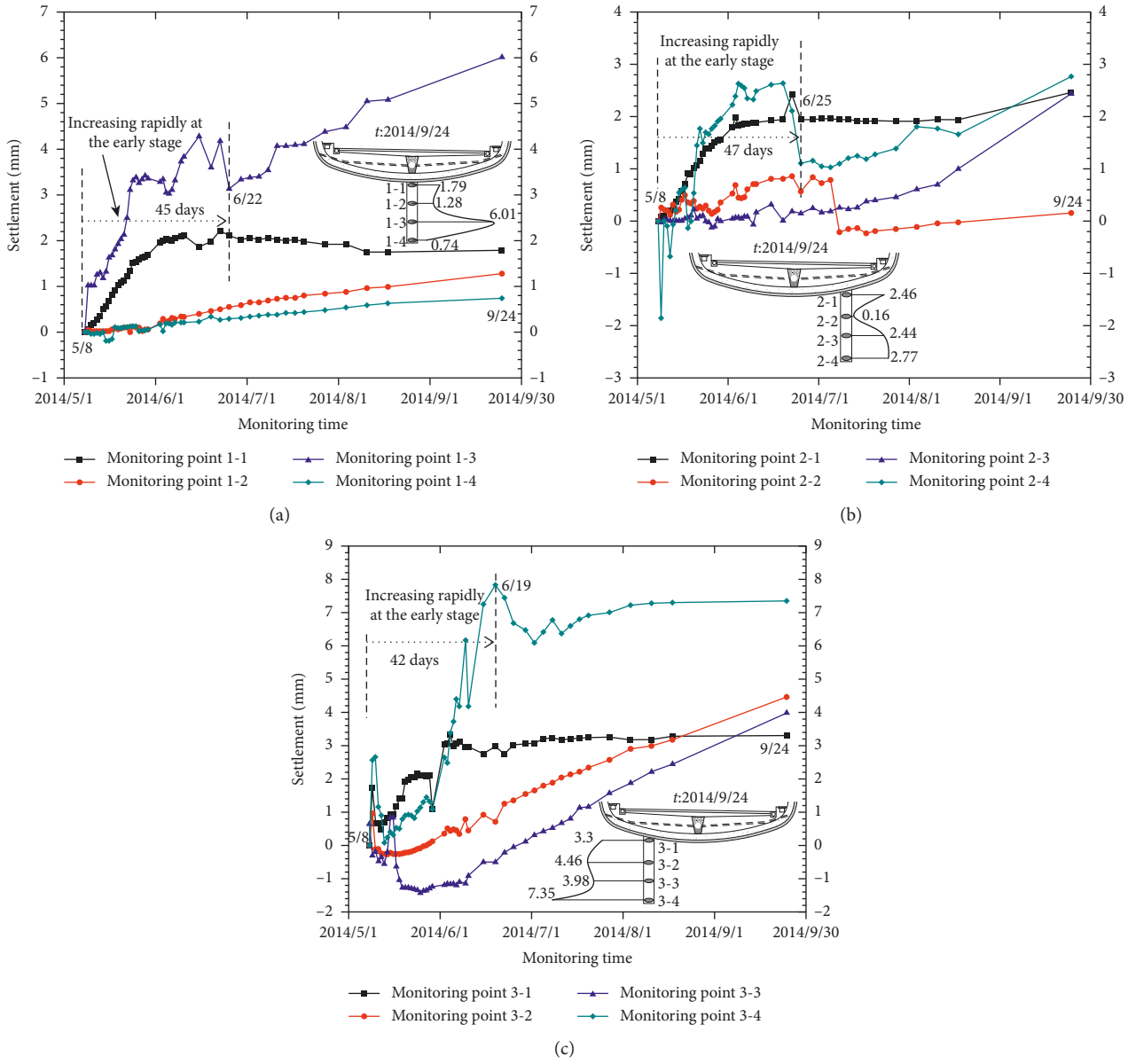

Figure 16: Variation of the settlement with time at the tunnel bottom. (a) Monitoring point 1. (b) Monitoring point 2. (c) Monitoring point 3.

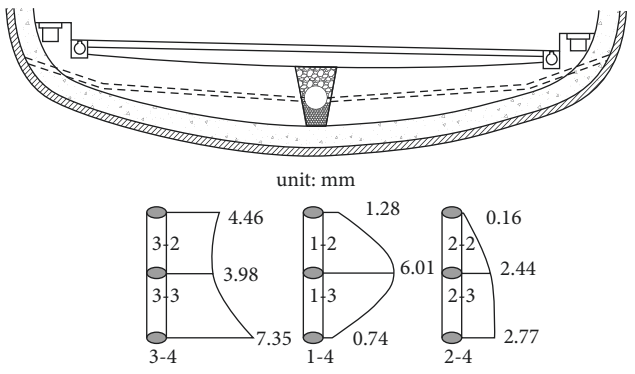

Figure 17: Settlement of tunnel foundations.

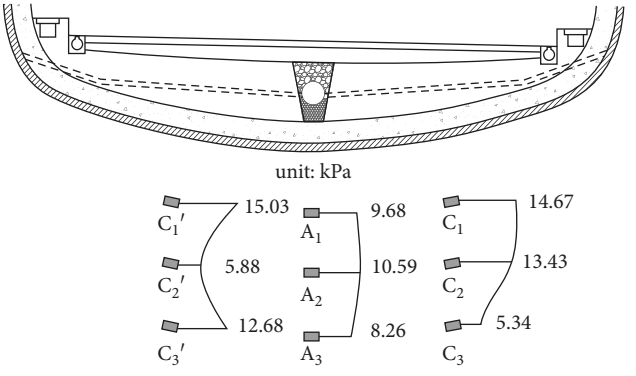

Figure 18: Additional stress of the tunnel foundation.

depth, which has a maximum settlement difference of 4.6 mm. The settlement of the reinforced foundation is uniformly distributed with no uneven settlement, and the jet grouting pile plays an important role in protecting the lining of the soft loess tunnel foundation.

Data Availability

The data used to support the findings of this study are available from the corresponding author upon request.

Conflicts of Interest

The authors declare that they have no conflicts of interest.

Acknowledgments

This work was financially supported by the Western Traffic Science and Technology Project (Grant No. 2014 318 J27 210), the Project on Social Development of Shaanxi Provincial Science and Technology Department (No. 2018SF-382), the Special Fund for Basic Scientific Research of Central Colleges of Chang'an University (Nos. 310821172004, 310821153312, and 310821165011), and the National Key R&D Program of China (No. 2018YFC0808700).

References

[1] J. X. Lai, S. Y. He, J. X. Chen et al., "Characteristics of seismic disasters and aseismic measures of tunnels in Wenchuan earthquake," *Environmental Earth Sciences*, vol. 76, no. 2, pp. 76–94, 2017.

[2] J. L. Qiu, X. L. Wang, S. Y. He, H. Q. Liu, J. X. Lai, and L. X. Wang, "The Catastrophic landside in Maoxian County, Sichuan, SW China, on June 24,2017," *Natural Hazards*, vol. 89, no. 2, pp. 1485–1493, 2017.

[3] Z. Q. Zhang, H. Y. Li, H. Y. Yang, and B. Wang, "Failure modes and face instability of shallow tunnels under soft grounds," *International Journal of Damage Mechanics*, 2018.

[4] X. Z. Li, C. Z. Qi, and Z. S. Shao, "A microcrack growth-based constitutive model for evaluating transient shear properties during brittle creep of rocks," *Engineering Fracture Mechanics*, vol. 194, pp. 9–23, 2018.

[5] J. B. Wang, Z. P. Song, B. Y. Zhao, X. R. Liu, J. Liu, and J. X. Lai, "A study on the mechanical behavior and statistical damage constitutive model of sandstone," *Arabian Journal for Science and Engineering*, vol. 43, no. 10, pp. 5179–5192, 2018.

[6] Y. Q. Wang, Z. F. Wang, and W. C. Cheng, "A review on land subsidence caused by groundwater withdrawal in Xi'an, China," *Bulletin of Engineering Geology and the Environment*, pp. 1–13, 2018.

[7] X. L. Luo, L. Y. Niu, and S. G. Zhang, "An algorithm for traffic flow prediction based on improved SARIMA and GA," *KSCE Journal of Civil Engineering*, pp. 1–9, 2018.

[8] Q. X. Yan, H. Chen, W. Y. Chen, J. C. Zhang, and X. Huang, "Dynamic characteristic and fatigue accumulative damage of a cross shield tunnel structure under vibration load," *Shock and Vibration*, vol. 2018, Article ID 9525680, 14 pages, 2018.

[9] W. H. Zhou, H. Y. Qin, J. L. Qiu et al., "Building information modelling review with potential applications in tunnel engineering of China," *Royal Society Open Science*, vol. 4, no. 8, pp. 170–174, 2017.

[10] J. X. Lai, X. L. Wang, J. L. Qiu et al., "A state-of-the-art review of sustainable energy based freeze proof technology for cold-region tunnels in China," *Renewable and Sustainable Energy Reviews*, vol. 82, pp. 3554–3569, 2018.

[11] X. X. Nie, X. B. Wei, X. C. Li, and C. W. Lu, "Heat treatment and ventilation optimization in a deep mine," *Advances in Civil Engineering*, vol. 2018, Article ID 1529490, 12 pages, 2018, In press.

[12] J. X. Lai, J. L. Qiu, H. B. Fan, J. X. Chen, and Y. L. Xie, "Freeze-proof method and test verification of a cold region tunnel employing electric heat tracing," *Tunnelling and Underground Space Technology*, vol. 60, pp. 56–65, 2016.

[13] R. Ren, S. S. Xu, Z. D. Ren et al., "Numerical investigation of particle concentration distribution characteristics in twin-tunnel complementary ventilation system," *Mathematical Problems in Engineering*, vol. 2018, Article ID 1329187, 13 pages, 2018.

[14] J. X. Lai, J. L. Qiu, J. X. Chen, H. B. Fan, and K. Wang, "New technology and experimental study on snow-melting heated pavement system in tunnel portal," *Advances in Materials Science and Engineering*, vol. 2015, Article ID 706536, 11 pages, 2015.

[15] J. L. Qiu, H. Q. Liu, J. X. Lai, H. P. Lai, J. X. Chen, and K. Wang, "Investigating the long-term settlement of a tunnel built over improved loessial foundation soil using jet grouting technique," *Journal of Performance of Constructed Facilities*, vol. 32, no. 5, 2018.

[16] Z. Wang, Z. Hu, J. Lai et al., "Settlement characteristics of jacked box tunneling underneath a highway embankment," *Journal of Performance of Constructed Facilities*, 2018.

[17] A. M. Assallay, C. D. F. Rogers, and I. J. Smalley, "Formation and collapse of metastable particle packings and open structures in loess deposits," *Engineering Geology*, vol. 48, no. 1-2, pp. 101–115, 1997.

[18] Q. G. Liang, J. Li, X. Y. Wu, and A. N. Zhou, "Anisotropy of Q2 loess in the Baijiapo tunnel on the Lanyu railway, China," *Bulletin of Engineering Geology and the Environment*, vol. 75, no. 1, pp. 109–124, 2016.

[19] J. X. Lai, J. L. Qiu, Z. H. Feng, J. X. Chen, and H. B. Fan, "Prediction of soil deformation in tunnelling using artificial neural networks," *Computational Intelligence and Neuroscience*, vol. 2016, Article ID 6708183, 16 pages, 2016.

[20] D. L. Zhang, Q. Fang, P. F. Li, and L. N. Y. Wong, "Structural responses of secondary lining of high-speed railway tunnel excavated in loess ground," *Advances in Structural Engineering*, vol. 16, no. 8, pp. 1371–1379, 2013.

[21] J. L. Qiu, X. L. Wang, J. X. Lai, Q. Zhang, and J. B. Wang, "Response characteristics and preventions for seismic subsidence of loess in Northwest China," *Natural Hazards*, vol. 92, no. 3, pp. 1909–1935, 2018.

[22] J. L. Qiu, Y. W. Qin, J. X. Lai et al., "Structural response of the metro tunnel under local dynamic water environment in loess strata," *Geofluids*, 2018, In press.

[23] Y. Luo, J. Chen, S. Gao, X. Deng, and P. Diao, "Stability analysis of super-large-section tunnel in loess ground considering water infiltration caused by irrigation," *Environmental Earth Sciences*, vol. 76, no. 22, 2017.

[24] Z. Wang, Y. Xie, J. Qiu, Y. Zhang, and H. Fan, "Field experiment on soaking characteristics of collapsible loess," *Advances in Materials Science and Engineering*, vol. 2017, Article ID 6213871, 17 pages, 2017.

[25] S. M. Haeri, A. Khosravi, A. A. Garakani, and S. Ghazizadeh, "Effect of soil structure and disturbance on hydromechanical behavior of collapsible loessial soils," *International Journal of Geomechanics*, vol. 17, no. 1, 2016.

[26] I. J. Smalley, ""In-situ" theories of loess formation and the significance of the calcium-carbonate content of loess," *Earth Science Reviews*, vol. 7, no. 2, pp. 67–85, 1971.

[27] E. Derbyshire, T. A. Dijkstra, I. J. Smalley, and Y. Li, "Failure mechanisms in loess and the effects of moisture content changes on remoulded strength," *Quaternary International*, vol. 24, pp. 5–15, 1994.

[28] C. D. F. Rogers, T. A. Dijkstra, and I. J. Smalley, "Hydro-consolidation and subsidence of loess: studies from China, Russia, North America and Europe: in memory of Jan Sajgalik," *Engineering Geology*, vol. 37, no. 2, pp. 83–113, 1994.

[29] Y. M. Reznik, "Influence of physical properties on deformation characteristics of collapsible soils," *Engineering Geology*, vol. 92, no. 1-2, pp. 27–37, 2007.

[30] Y Fang, Z. G. Yao, G. Walton, and Y. P. Fu, "Liner behavior of a tunnel constructed below a caved zone," *KSCE Journal of Civil Engineering*, pp. 1–10, 2018.

[31] Q. X. Yan, L. Y. Song, H. Chen, W. Y. Chen, S. Q. Ma, and W. B. Yang, "Dynamic response of segment lining of overlapped shield tunnels under train-induced vibration loads," *Arabian Journal for Science and Engineering*, vol. 43, no. 10, pp. 5439–5455, 2018.

[32] H. J. Zhang, Z. Z. Wang, F. Lu, G. Y. Xu, and W. G. Qiu, "Analysis of the displacement increment induced by removing temporary linings and corresponding countermeasures," *Tunnelling and Underground Space Technology*, vol. 73, pp. 236–243, 2018.

[33] J. X. Lai, J. L. Qiu, H. B. Fan et al., "Fiber Bragg grating sensors-based in-situ monitoring and safety assessment of loess tunnel," *Journal of Sensors*, vol. 2016, Article ID 8658290, 10 pages, 2016.

[34] S. J. Feng, F. L. Du, Z. M. Shi, W. H. Shui, and K. Tan, "Field study on the reinforcement of collapsible loess using dynamic compaction," *Engineering Geology*, vol. 185, pp. 105–115, 2015.

[35] W. Feng, R. Huang, and T. Li, "Deformation analysis of a soft–hard rock contact zone surrounding a tunnel," *Tunnelling & Underground Space Technology Incorporating Trenchless Technology Research*, vol. 32, no. 11, pp. 190–197, 2012.

[36] Z. Q. Zhang, X. Q. Shi, B. Wang, and H. Y. Li, "Stability of NATM tunnel faces in soft surrounding rocks," *Computers and Geotechnics*, vol. 96, pp. 90–102, 2018.

[37] Z. F. Wang, Y. Q. Wang, and W. C. Cheng, "Investigation into Geohazards during Urbanization Process of Xi'an, China," *Natural Hazards*, vol. 92, no. 3, pp. 1937–1953, 2018.

[38] Y. Li, Y. Yang, H. Yu, and G. Roberts, "Principal stress rotation under bidirectional simple shear loadings," *KSCE Journal of Civil Engineering*, vol. 22, no. 5, pp. 1651–1660, 2018.

[39] G. Meschke, J. Ninić, J. Stascheit, and A. Alsahly, "Parallelized computational modeling of pile–soil interactions in mechanized tunneling," *Engineering Structures*, vol. 47, no. 1, pp. 35–44, 2013.

[40] S. Seki, S. Kaise, Y. Morisaki, S. Azetaka, and Y. Jiang, "Model experiments for examining heaving phenomenon in tunnels," *Tunnelling and Underground Space Technology*, vol. 23, no. 2, pp. 128–138, 2008.

[41] C. J. Lee, B. R. Wu, H. T. Chen, and K. H. Chiang, "Tunnel stability and arching effects during tunneling in soft clayey soil," *Tunnelling and Underground Space Technology*, vol. 21, no. 2, pp. 119–132, 2006.

[42] H. He, Y. Lin, J. Li, and N. Zhang, "Immersed tunnel foundation on marine clay improved by sand compaction piles," *Marine Georesources and Geotechnology*, vol. 36, no. 2, pp. 218–226, 2017.

[43] H. E. Ben, L. Z. Wang, and Y. Hong, "Capacity and failure mechanism of laterally loaded jet-grouting reinforced piles: field and numerical investigation," *Science China Technological Sciences*, vol. 59, no. 5, pp. 763–776, 2016.

[44] J. Z. Hao, C. G. Wu, and Y. Liu, "Economic and technical analysis of foundation reinforcement scheme for Dayoushan tunnel," *Traffic Science and Technology in Qinghai*, vol. 2, pp. 28–30, 2012.

[45] GB50025-2004, *Code for Building Construction in Collapsible Loess Regions*, China Architecture and Building Press, Beijing, China, 2004.

[46] GB 50007-2002, *Code for Design of Building Foundation*, China Architecture and Building Press, Beijing, China, 2002.

[47] J. X. Lai, S. Mao, J. L. Qiu et al., "Investigation progresses and applications of fractional derivative model in geotechnical engineering," *Mathematical Problems in Engineering*, vol. 2016, Article ID 9183296, 15 pages, 2016.

[48] D70-2004 JTG, *Code for Design of Highway Tunnel*, China Communications Press, Beijing, China, 2004.

[49] E. Derbyshire, "Geological hazards in loess terrain, with particular reference to the loess regions of china," *Earth Science Reviews*, vol. 54, no. 1–3, pp. 231–260, 2001.

[50] Z. Liu, F. Liu, F. Ma et al., "Collapsibility, composition, and microstructure of loess in china," *Canadian Geotechnical Journal*, vol. 53, no. 4, pp. 673–686, 2016.

[51] P. Li, S. Vanapalli, and T. Li, "Review of collapse triggering mechanism of collapsible soils due to wetting," *Journal of Rock Mechanics and Geotechnical Engineering*, vol. 8, no. 2, pp. 256–274, 2016.

[52] Y. C. Gu, *Research on stress and deformation performance of jet pile composite foundation in deep and large section loess tunnel*, Ph.D. thesis, Chang' an University, Xi' an, China, 2015, in Chinese.

[53] S. J. Shao, J. Li, G. L. Li et al., "Evaluation method for self-weight collapsible deformation of large thickness loess foundation," *Chinese Journal of Geotechnical Engineering*, vol. 37, no. 6, pp. 966–978, 2014, in Chinese.

[54] X. L. Wang, Y. P. Zhu, and X. F. Huang, "Field tests on deformation property of self-weight collapsible loess with large thickness," *International Journal of Geomechanics*, vol. 14, no. 3, pp. 613–624, 2014.

[55] Q. X. Yan, B. J. Li, Z. X. Deng, and B. Li, "Dynamic responses of shield tunnel structures with and without secondary lining upon impact by a derailed train," *Structural Engineering and Mechanics*, vol. 65, pp. 741–750, 2018.

[56] D. M. Zhang, L. X. Ma, H. W. Huang, J. Zhang, N. Thai-Quang, and N. Mai-Duy, "Predicting leakage-induced settlement of shield tunnels in saturated clay," *Computer Modeling in Engineering and Sciences*, vol. 89, no. 89, pp. 163–188, 2012.

[57] J. X. Lai, K. Y. Wang, J. L. Qiu, F. Y. Niu, J. B. Wang, and J. X. Chen, "Vibration response characteristics of the cross tunnel structure," *Shock and Vibration*, vol. 2016, Article ID 9524206, 16 pages, 2016.

[58] P. F. Li, Y. Zhao, and X. J. Zhou, "Displacement characteristics of high-speed railway tunnel construction in loess ground by using multi-step excavation method," *Tunnelling and Underground Space Technology*, vol. 51, pp. 41–55, 2016.

[59] Z. Wang, Y. Xie, H. Liu et al., "Analysis on deformation and structural safety of a novel concrete-filled steel tube support system in loess tunnel," *European Journal of Environmental and Civil Engineering*, 2018.